IMPORTANCE OF SECONDARY BENDING EVALUATION IN STRUCTURAL JOINT

Dr. Willy Roger de Paula Mendonça
Embraer S.A.
Keywords: *severity factor, secondary bending, fatigue, joint*

Abstract

This study proposes a new methodology for fuselage structural joint analysis. The new methodology includes the geometric nonlinearity effects in joints, which influence the secondary bending stress. Changing the traditional methods analysis by adding secondary bending stress to the resultant normal stress used to calculate joint severity factor (SF), shows that the SF for fatigue analysis is a function of the loading applied. In other words, the SF is variable and not constant as usually applied in traditional analysis methods. In this study, a pre-design software was developed, and was verified by experimental results from a number of joint designs. These results are presented in this study in order to demonstrate the importance of evaluating the secondary bending for correct predicting fatigue behavior.

1 Introduction

This study proposes a methodology developed to generate pre-sizing fatigue curves for typical fuselage structural joints (lap, butt, and stepped butt joints).

A thorough understanding of the stresses at the most critical fastener row is essential when conducting fatigue and damage tolerance analyses of mechanically fastened joints. The critical fastener row location is most susceptible to fatigue crack nucleation and subsequent crack growth [1].

The developed methodology applied analytical models to obtain the stress components (tensile and bending) for different joint designs, and through these stresses estimates the severity factor (SF) for the critical fastener row. The SF result is calculated from the specific stress concentration factors (kts) for each stress component.

Because of the nonlinear geometry in the joints, when a tensile stress is applied, it generates a secondary out-of-plane bending loading. The ratio between tensile and flexural stresses is variable, i.e., non-linear, resulting in a non-linear SF, as shown in Fig. 1.

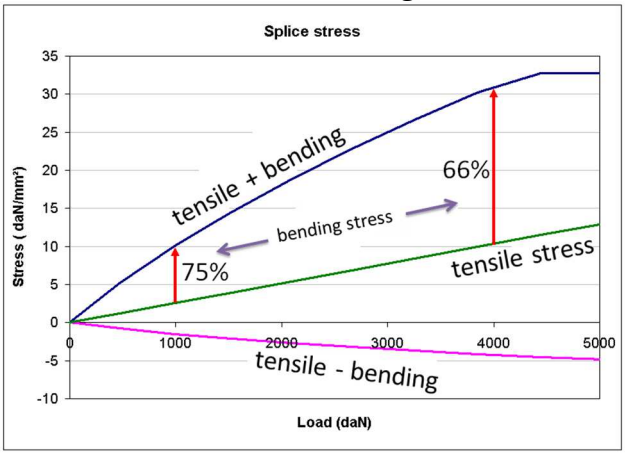

Fig. 1 – Bending stress ratio

The SF is function of the applied stress level. Typically, a greater SF is observed for smaller stress loadings as, in this situation, there is a greater proportion of bending stress in the total stress, as shown in Fig. 2.

An important aspect that will be shown in this study is that the critical fastener row, where fatigue failure occurs in joints, is a function of design and the applied level of loading. Therefore, it is possible to assert that failures can be predicted in different fastener rows for the same joint, if the applied loading level is known. This failure fastener row shift was observed experimentally, in a number of

tested designs, and also was reported in the scientific papers [2].

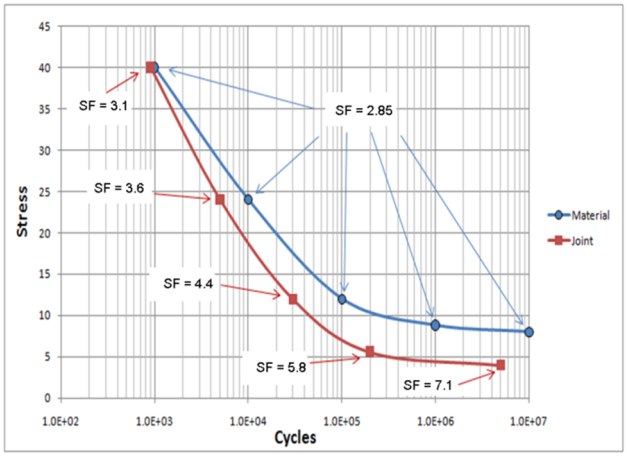

Fig. 2 – Variable SF for nonlinear analysis

Figure 3 shows the fatigue curves obtained for three different joints, which were grouped due to the level of similarity between them. This graph allows visualization of the effects of small design differences in fatigue curve behavior.

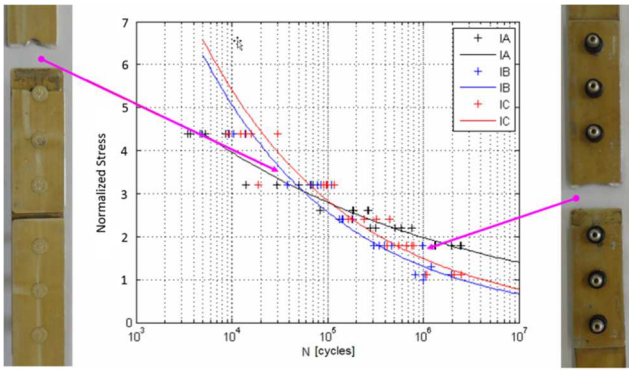

Fig. 3 – Section failure in joint design IB

Photographs of failure specimens are shown on either side of the graph. These failures were obtained during the fatigue test. The arrows in Fig. 3 indicate in the IB-curve the stress level at which they were tested; it is observed that the failures occurred in different sections.

Correctly identifying the fastener row that would have failed in the joint is only possible when considering the effects of the secondary bending that occurs at a given loading. The methodology presented in this study makes this prediction possible.

In section 2, the development of the analysis methodology will be presented. In section 2.1 the analytical deductions used to obtain the stress acting in the fastener row sections for the three typical fuselage designs are presented. The analytical models used have been widely proven in the literature and are based on the neutral line model (NLM) [3-7].

In section 2.2, the analysis methodology flowchart is presented. This provides details of the analysis steps required. Software was developed during the study to add secondary bending effects into the analysis. It was focused on simplifying the joint analysis process, increasing productivity by process automation, and eliminating preliminary analyses, including the calculation of fastener stiffness, transfer loads of fasteners, and stress concentration factors.

In order to correlate the analytical methodology, finite element analyses (FEA) were developed. FEA is able to evidenced effects as secondary bending more easily, but that required an analysis somewhat more complex and slower than the study proposal.. The FEA worked as a virtual test for the correlations presented in section 2.3. In order to support these simulations a number of experimental tests were performed.

In section 3, the validation of the software results is presented. The stress correlations from the stresses calculated by the analytical models, the FEA, and also acquired from tests performed are presented in section 3.1. A second correlation will be presented in section 3.2 by a comparison of the joint fatigue curves from the simulated and experimental results.

And finally, considerations regarding the use of the software will be discussed, and the improvements obtained with respect to the methodologies that do not consider the nonlinearity of the joints will be evaluated with the results of the correlations.

2 Development

The development comprised adding the nonlinear behavior of typical fuselage joint

designs to existing analytical methodologies based on linear models.

First, the neutral line equations were deduced for the three selected fuselage joint designs. The deductions were developed from the bibliography review, and were added to when necessary. At this stage the formulation for the tensile and secondary bending stresses for the joints was consolidated.

It was observed that the application of this methodology could potentially simulate joint fatigue curves. In order to realize this, it would be necessary to create software that automates a number of preliminary analyses. The software developed apply analytical tools with methodologies presented in the literature [8], adapting them to include the nonlinear behavior of the joints.

The final stage of the development comprised validating the results obtained by the software. The first correlation was for the simulated joint stresses, the FEA results, and experimental measurements obtained by extensometers in the static tests. The second correlation was performed by comparing the fatigue curves obtained from a number of tests performed by EMBRAER and the fatigue curves simulated by the software.

2.1 The neutral line model deduction for joint models

The analytical models used in this analysis were aimed at enabling fast and efficient execution of preliminary analyses. The models presented are based on the NLM.

The neutral line deflection occurs because of eccentricity in the joint geometry. To obtain the joint neutral line deflection, it is necessary to solve the differential equation that represents the analyzed segment. The same procedure for the development of NLM was used for all three joint types presented in this study.

The NLM deduction for a lap-joint is presented first. As the deduction for the butt-joint is similar it will not be described in detail, and only the model used and the equations system used to obtain the neutral line are presented.

2.1.1 NLM for lap joints

An NLM is unidirectional and the response of a structure to an excitation force is restricted to the behavior of its neutral line. The lap joint and the nomenclature are shown in Fig. 4. The edges were clamped for all models considered. The deflection of the neutral line of this joint is shown in Fig. 5.

The stress calculation in the critical fastener row is discussed below, starting with the static equilibrium evaluation of the joint.

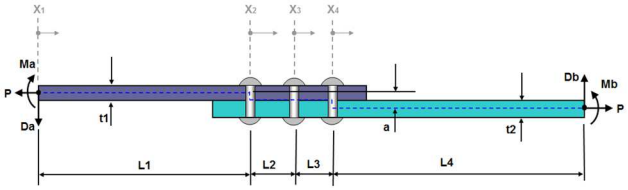

Fig. 4 – Nomenclature for lap joint geometry

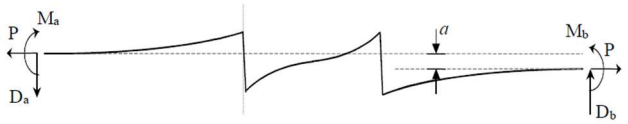

Fig. 5 – NLM with out-of-plane displacement

$$\sum M_{point\ A} = 0 \tag{1}$$

$$M_a - M_b - P.a - D_b.L_{tot} = 0 \tag{2}$$

$$L_{tot} = L_1 + L_2 + L_3 + L_4 \tag{3}$$

The equilibrium for each separate "beam" segment can be written as follows:

$$(M_x)_i = M_a + P.w_i - D_a.\left(\sum_{i=1}^{4} L_{i-1} + x_i\right) = (EI)_i.\left(\frac{d^2w}{dx^2}\right)_i \tag{4}$$

Or, in a more useful form:

$$\left(\frac{d^2w}{dx^2}\right)_i - \alpha_i^2.w_i = \alpha_i^2.\left(\frac{M_a}{P} - \frac{D_a}{P}.\left(\sum_{i=1}^{4} L_{i-1} + x_i\right)\right) \tag{5}$$

with

$$\alpha_i^2 = \frac{P}{(EI)_i} \tag{6}$$

where

P = Remote applied axial load;

Ma = Moment from clamping;
Da = Reaction force from clamping;
Ei =Modulus of elasticity for the ith segment of the beam; and
Ii = Moment of inertia for the ith segment of the beam;

Solving Eq. (5) yields a second-order linear equation for the ith "beam" segment.

$$w_i = A_i.\sinh(\alpha_i.x_i) + B_i.\cosh(\alpha_i.x_i) + \left(\frac{D_a}{P}\left(\sum_{i=1}^{4} L_{i-1} + x_i\right) - \frac{M_a}{P}\right) \quad (7)$$

The boundary conditions for the position of the fasteners are as follows:

$$w_i + e_i = w_{i+1} \;\; and \;\; \left(\frac{dw}{dx}\right)_i = \left(\frac{dw}{dx}\right)_{i+1} \quad (8)$$

Therefore, a system with 10 equations and 10 unknowns, as shown in Tab. 1, must be solved.

Solving the equations system yields the neutral line displacement at any point "x" along the joint. The bending moment can be calculated by Eq. (9).

$$M_x = M_a + P.w_x - D_a.L_x \quad (9)$$

Tab. 1 – Lap joint equation system

$A_1 = -\frac{D_a}{\alpha_1.P}$
$B_1 = \frac{M_a}{P}$
$B_2 = A_1.\sinh(\alpha_1.L_1) + B_1.\cosh(\alpha_1.L_1) + e_1$
$A_2.\alpha_2 = A_1.\alpha_1.\cosh(\alpha_1.L_1) + B_1\alpha_1.\sinh(\alpha_1 L_1)$
$B_3 = A_2.\sinh(\alpha_2.L_2) + B_2.\cosh(\alpha_2.L_2) + e_2$
$A_3.\alpha_3 = A_2.\alpha_2.\cosh(\alpha_2.L_2) + B_2\alpha_2.\sinh(\alpha_2 L_2)$
$B_4 = A_3.\sinh(\alpha_3.L_3) + B_3.\cosh(\alpha_3.L_3) + e_3$
$A_4.\alpha_4 = A_3.\alpha_3.\cosh(\alpha_3.L_3) + B_3\alpha_3.\sinh(\alpha_3 L_3)$
$A_4.\sinh(\alpha_4.L_4) + B_4.\cosh(\alpha_4.L_4) + \left(\frac{D_a}{P}.L_{tot} - \frac{M_a}{P}\right) = a$
$A_4.\alpha_4.\cosh(\alpha_4.L_4) + B_4\alpha_4.\sinh(\alpha_4 L_4) + \frac{D_a}{P} = 0$

Equation (10), is used to calculate the bending stress:

$$\sigma_b(y) = \frac{M_x.y}{I_x} \quad (10)$$

Where "y" is the distance between the point of interest in the thickness and the neutral line.

2.1.2 NLM for butt joints

The analytical model deduced for the butt joints (Figs. 6 and 7) integrates the equations system presented in Tab 2.

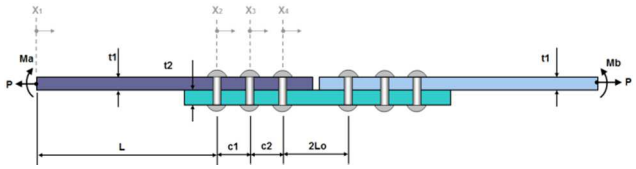

Fig. 6 – Nomenclature for butt joint

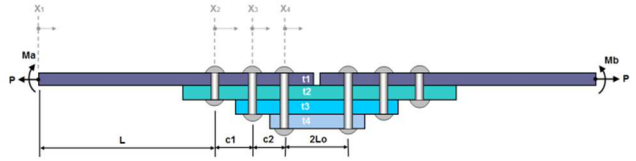

Fig. 7 – Nomenclature for stepped butt joint

where:

$$e_1 = \frac{t_1}{2} - \frac{(t_1 + t_2)}{2},\; e_2 = \frac{(t_1 + t_2 + t_3)}{2} - \frac{(t_1 + t_2)}{2},$$
$$e_3 = t_1 + \frac{(t_2 + t_3 + t_4)}{2}$$

Tab. 2 – Butt joint equation

$A_1.\alpha_1 = 0$
$B_1 = \frac{M_a}{P}$
$B_2 = A_1.\sinh(\alpha_1.L) + B_1.\cosh(\alpha_1.L) + e_1$
$A_2.\alpha = A_1.\alpha_1.\cosh(\alpha_1.L) + B_1.\alpha_1.\sinh(\alpha_1 L)_2$
$B_3 = A_2.\sinh(\alpha_2.c_1) + B_2.\alpha_2.\sinh(\alpha_2.c_1) + e_2$
$A_3.\alpha = A_2.\alpha_2.\cosh(\alpha_2.c_1) + B_2.\alpha_2.\sinh(\alpha_2.c_1)_3$
$B_4 = A_3.\sinh(\alpha_3.c_2) + B_3.\cosh(\alpha_3.c_2) + e_3$
$A_4.\alpha_4 = A_3.\alpha_3.\cosh(\alpha_3.c_2) + B_3.\alpha_3.\sinh(\alpha_3.c_2)$
$A_4.\alpha_4.\cosh(\alpha_4.L_0) + B_4.\alpha_4.\sinh(\alpha_4.L_0) = 0$

2.2 Software for analysis, predesign, and performance evaluation

Software was developed to generate fatigue curves for a number of joint designs presented in this study. Other analysis tools, with

methodologies presented in the literature [8], were adapted and incorporated in this software, thereby decreasing the number of stages in the analysis process. Figure 8 shows the flowchart of the algorithm developed for the fatigue curve prediction.

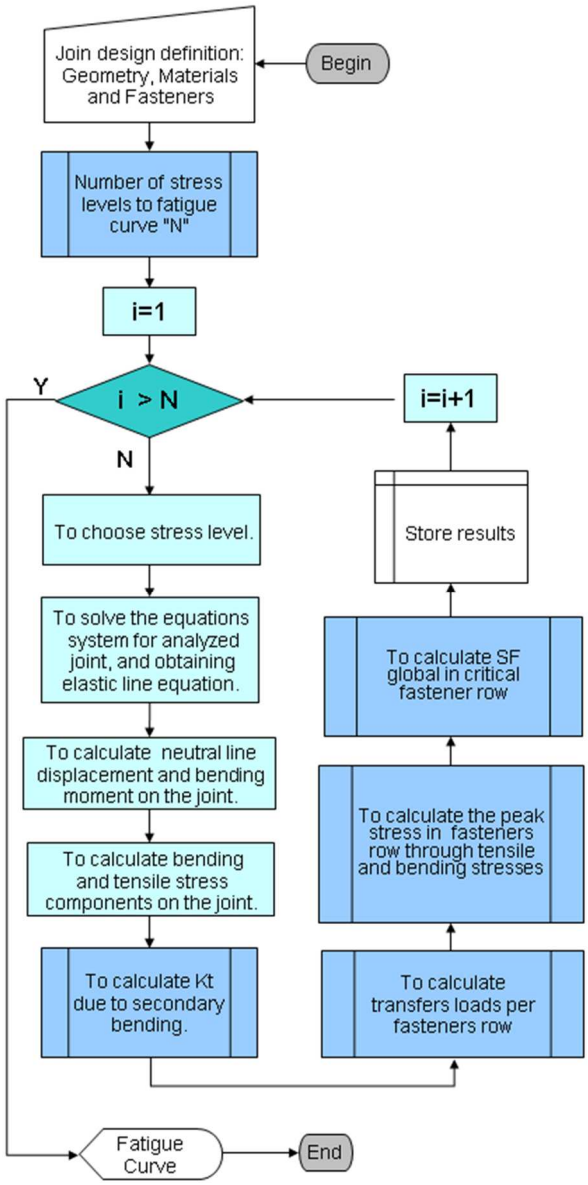

Fig. 8 – Nonlinear analysis flowchart

2.3 Finite element analysis for correlations

Different finite element models (FEM) can be used for joint analyses. The complexity of the model used is determined by the level of representativeness required for the analysis, which could differ depending on the stage of development of the project or the importance of the joint.

The models developed were aimed at verifying the stresses on the joint parts, simulated by the analytical model. The FEA model required only moderate representativeness and was developed with the NASTRAN elements in order to correlate with the software results.

Simplified models are built with: coincident nodes, coarse refinement, and shell elements. At the other extreme, the complex models use solid elements for parts and considered the clamp force of the contact between the parts and fasteners.

The FEM developed is shown in Fig. 9. It used QUAD4 elements with a size equivalent to the diameter of the fasteners to represent the splice parts. For the connection between the splices, CFAST elements were used with the stiffness of the respective fasteners. In order to load the model, it was used the RBE2 element, that distributes the loading on one edge of the model.

The actual offset between the joint components was included. The boundary conditions were represented by clamped edges. NASTRAN SOL106, which is designed for nonlinear analyses, was used to solve the simulation.

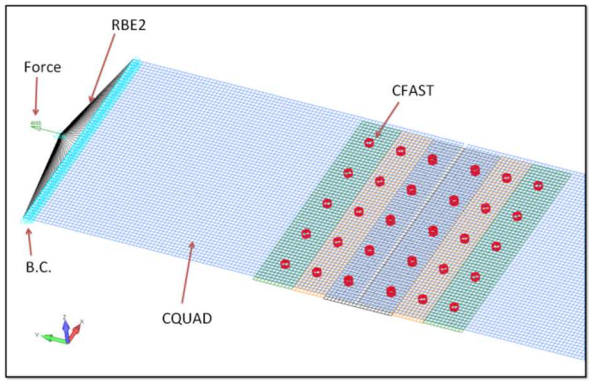

Fig. 9 – Butt joint finite element model

3 Results

In this section the correlations developed to verify the analytical simulations are presented. In section 3.1, the stress joint correlations are presented. The comparative results were obtained analytically by the software, experimentally, and numerically by FEA.

In section 3.2 the experimental results are presented for the fatigue curve fitting. These

results are compared with the software-simulated curves that used the nonlinear models and a simulated curve with the more traditional methodology using linear analytical models.

3.1 Stress correlation

The correlation results are presented for each joint design studied. The joint designs and experimental results presented in this section are derived from both the Rijck thesis [7] and development carried out at EMBRAER.

Correlations were made by comparing the stresses obtained by the three methods (analytical, numerical, and experimental). In all correlation graphs, the stresses presented refer to one of the specimens faces: TOP (top face) or BOT (bottom face).

The experimentally measured strains were obtained for the sections of interest on the specimens. The strains were converted to stress using the unidirectional Hooke's law. The stresses measured were the total normal stresses, that is the resultant of the tensile and bending stress components. Table 3 presents a list of the joints correlated in this paper, the thicknesses of the splices, and the experimental results references.

Tab. 3 – Correlated joints

Specimen	Thickness [mm]	Reference
Lap joint	t1 = 4.0	Rijck. 2007
	t2 = 4.0	
Butt joint	t1 = 2.5	Rijck. 2007
	t2 = 2.0	
Stepped butt joint	t1= 3.0	Embraer
	t2 = 2.0	
	t3 = 2.5	
	t4 = 3.8	

3.1.1 Stepped butt joint stress correlation

In this section the correlations for the stepped butt joint are presented. The specimen geometry is shown in Fig. 10.

Fig. 10 – Static tested stepped butt joint

The stress results from the FEA used in the correlation are shown in Figs. 11–14, and correlations of the stress results obtained by the three methods are shown in Figs. 14 and 15.

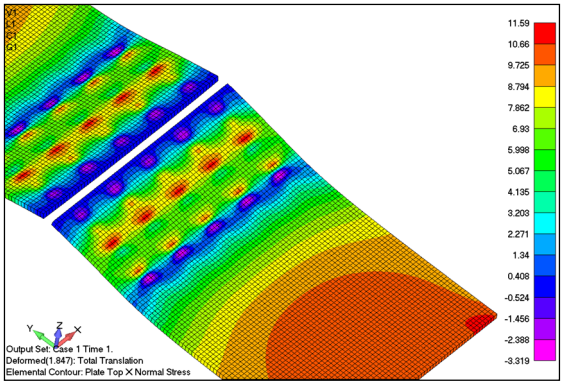

Fig. 11 – Skin stress – TOP side

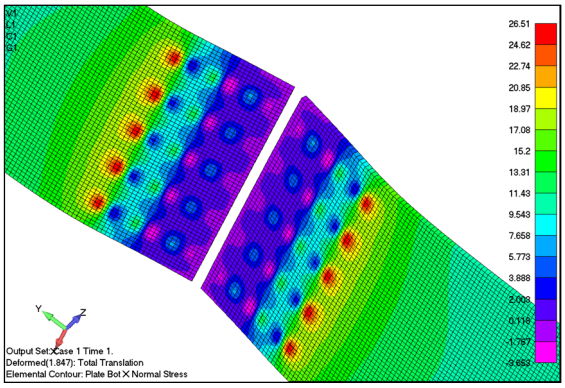

Fig. 12 – Skin stress – BOT side

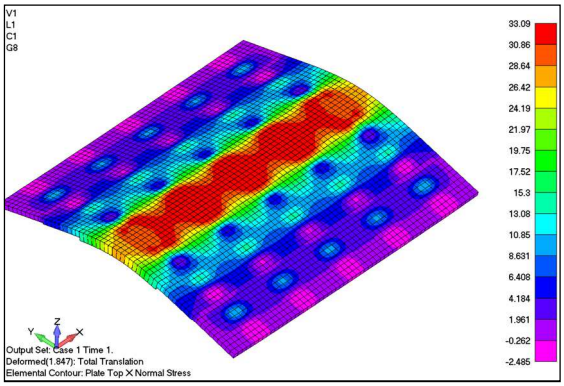

Fig. 13 – Splice stress – TOP side

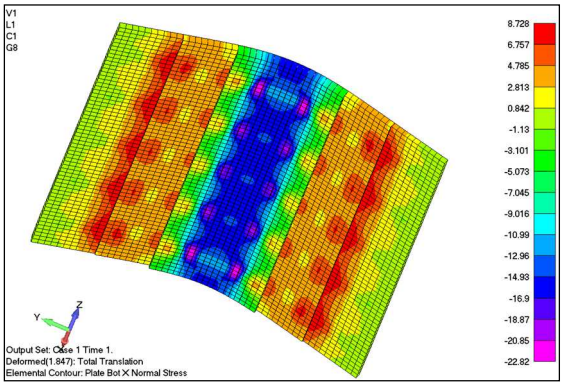

Fig. 14 – Splice stress – BOT side

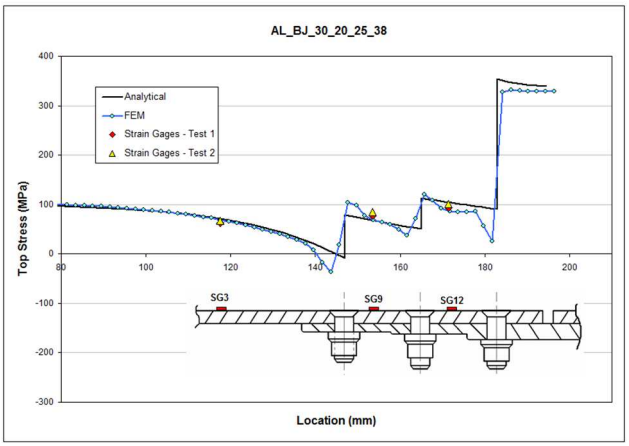

Fig. 15 – Stress correlation - TOP side

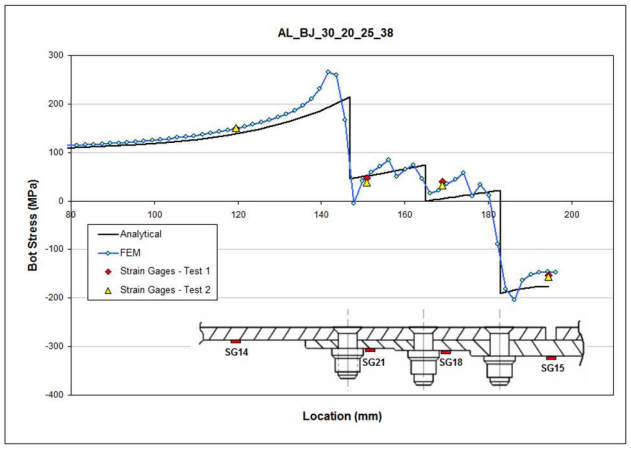

Fig. 16 – Stress correlation – BOT side

3.1.2 Butt joint stress correlation

In this section the correlation for butt joints is presented. Graphs correlating the stress results obtained by the three methods are shown in Figs. 17 and 18.

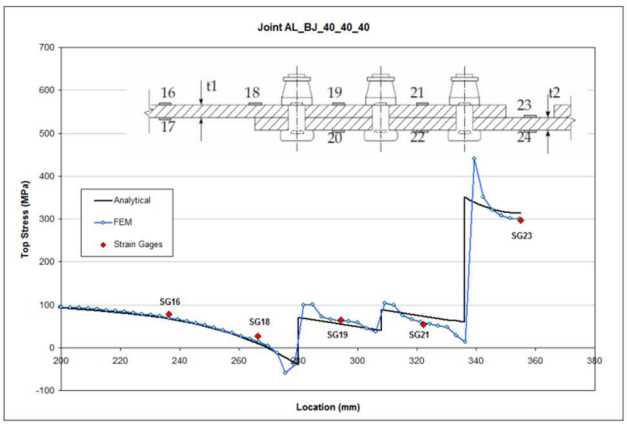

Fig. 17 – Stress correlation – TOP side

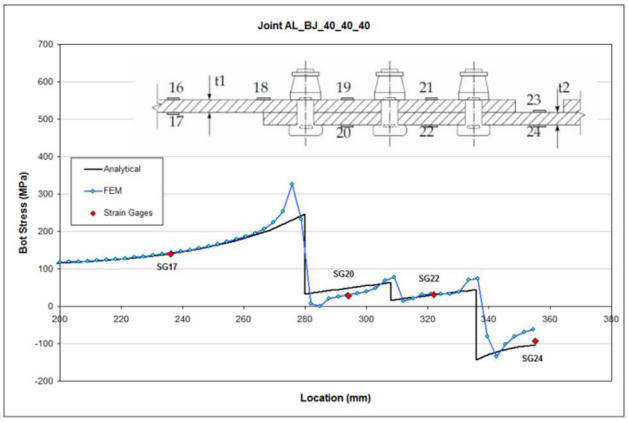

Fig. 18 – Stress correlation – BOT side

3.1.3 Lap joint stress correlation

In this section the correlation for lap joints are presented. A graph correlating the stress results obtained by the three methods is shown in Fig. 19. This joint is symmetrical and, for this reason, only one side was correlated.

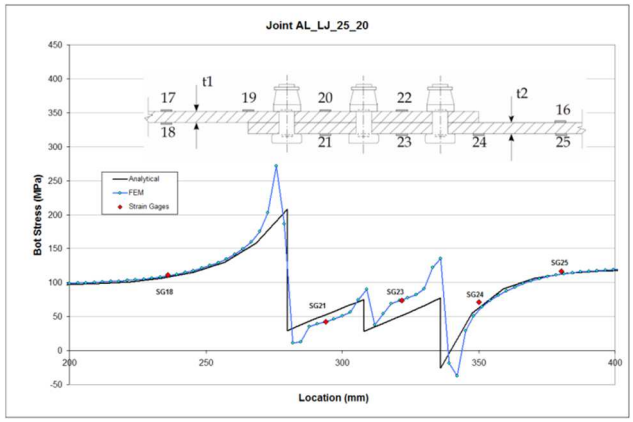

Fig. 19 – Stress correlation – BOT side

3.2 Fatigue curves correlation (Analytical vs. Experimental)

In this section the correlations from the fatigue curves are presented. Analyses were performed for different joint designs tested at EMBRAER. Table 4 presents the primary joint characteristics. The names in the "id" column correspond to the nomenclature used in the source reports.

On the correlation graphs the experimental results are represented as dots, the simulated fatigue curves by green lines, and the traditional linear analysis (Niu method) by blue lines.

The experimental stresses shown in the graphs were obtained from the applied loads and the net section areas.

The analytical curves were obtained by correcting the joint material fatigue curves by the critical SF for each stress level. The recommended fatigue curve to corrections are those obtained for an open hole, where kt = 2.85.

It is important to note that the SF obtained by the linear method is constant for any loading level, therefore, it is clear that it is only a linear function of the geometry. For the new methodology SF is variable because of the non-linearity of the joints.

All joint designs in Table 4 were analyzed and correlated. A selection of the specimens manufactured for the fatigue tests are shown in Fig. 20.

Four analyses were selected to demonstrate that linear analysis is not conservative in a number of joint designs and the proposed method was more efficient in predicting fatigue curves.

Tab. 4 – Joint design evaluated

Design	Configuration				
	id	skin (mm)	strap (mm)	Fastener / Rivet	Material
Butt	I_A	1.6	2	MS14218AD-5	AA2524-T3
Butt	I_B	1.6	2	HST11BJ-5	AA2524-T3
Butt	I_C	1.6	2	HST11BJ-5	AA2524-T3
Butt_scarf	II	3	2-2.5-3.8	HST11BJ-6	AA2524-T3
Lap	III_A	2	2	HST11BJ-5	AA2524-T3
Lap	III_B	2	2	HST11BJ-5	AA2198-T851
Lap	-403	3.2	3.2	HST11BJ-6	AA2524-T3
Lap	-405	2	2	HST11BJ-5	AA2524-T3
Lap	-407	3.2	3.2	HST11BJ-5	AA2024-T3
Lap	-409	3.2	3.2	HST11BJ-5	AA7475
Lap	-411	3.2	3.2	HST11BJ-5	AA2524-T3
Lap	-413	3.2	3.2	HST11BJ-6	AA2524-T3
Lap	-415	3.2	3.2	HST11BJ-5	AA2524-T3
Lap	-417	3.2	3.2	LGPL2-5	AA2524-T3
Lap	-419	3.2	3.2	HST11BJ-5	AA2524-T3
Butt	cdp 3	1.6	1.778	PE26118-AD5	AA2524-T3
Butt	cdp 4	1.6	1.778	PE26118-AD5	AA2524-T3
Butt	cdp 5	1.6	1.778	PE26118-AD5	AA2524-T3
Butt_scarf	CF2 x CF3	2	2-2.5-3.8	HST11BJ-5	AA2524-T3
Butt	joint 2	1.6	2	MS14218-AD5	AA2024-T3
Butt	joint 4	2	2.54	MS14218-AD5	AA2024-T3
Butt	joint 2524	2	2.54	MS14218-AD5	AA2524-T3
Butt	central III	1.6	1.6	MS14218-AD5	AA2024-T42
Lap	lap 1	1.6	1.6	MS14218-AD5	AA2024-T3
Lap	171-17939-401	1.6	1.6	MS20470AD5-6	AA2524-T3
Lap	171-17941-401	1.6	1.6	MS14218AD5-5	AA2524-T3
Butt	171-17942-401	1.6	2	MS20470AD5-7	AA2524-T3
Butt	171-17943-401	1.6	2	MS14218AD5-5	AA2524-T3

These correlations are shown in Figs. 20–24, and Fig. 25 shows the variation of the critical SF as a function of the applied stress on one butt joint.

Evaluations of the other results, that are not presented in this study, indicated that the linear method was better able to fit the lap joint designs.

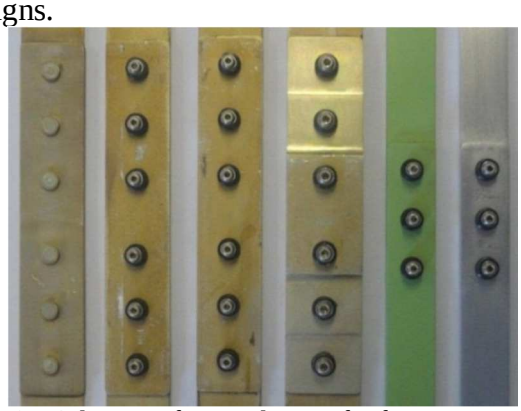

Fig. 20 – Selection of joints designs for fatigue testing

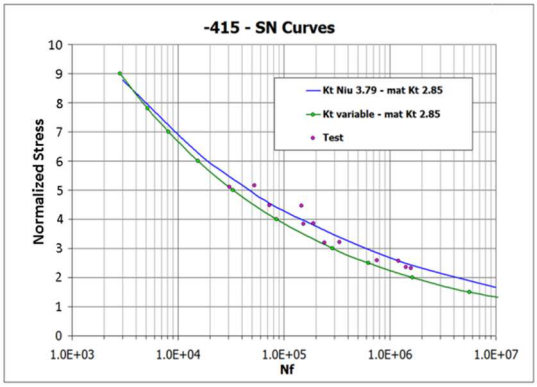

Fig. 21 – Fatigue curve correlation for lap joint

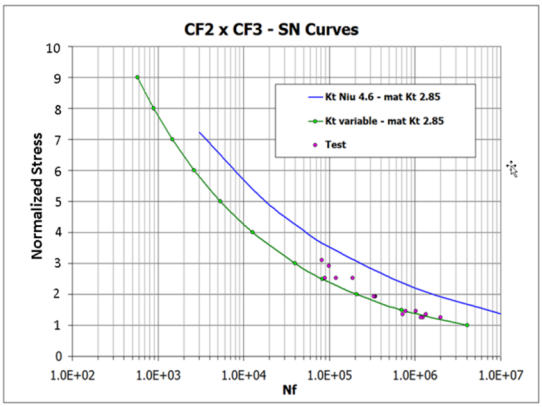

Fig. 22 – Fatigue curve correlation for butt stepped joint

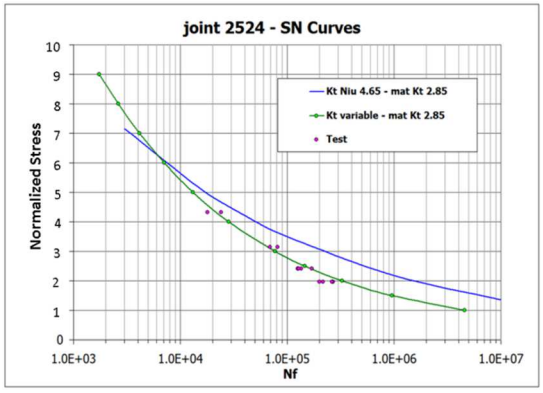

Fig. 23 – Fatigue curve correlation for butt joint

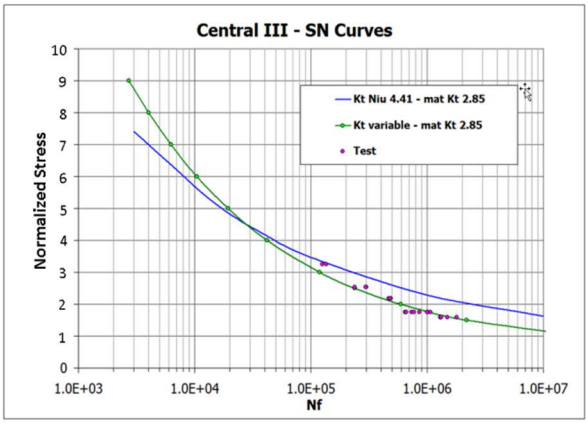

Fig. 24 – Fatigue curve correlation for butt joint

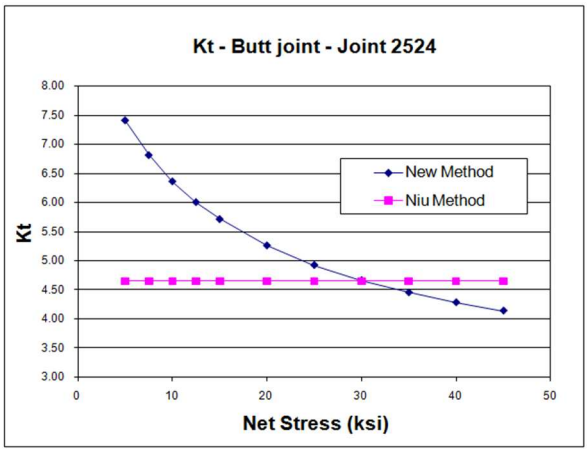

Fig. 25 – SF for butt joint

4 Comments and conclusions

The correlations presented in this study showed good results regarding the estimation of normal stresses for different joint designs. The stresses estimated by the analytical method were validated by two different techniques: FEA and experimental tests. Because of the few parameters required to use the software, this tool is faster than an FEA, and, with the implementation of a limited number of additional routines, a joint optimizer could be created.

The primary results of this study are the correlations made to obtain the joint fatigue curves. The correlations showed that the nonlinear method correctly predicted the fatigue curves of the three joint designs. For nine joint designs evaluated, of those listed in Tab. 4, adding the secondary moment was critical. In these cases, the linear method was not conservative. The simulation results were validated within a range of thicknesses, materials, and fasteners typically found in a fuselage. For joints with greater thicknesses than these, as observed in wings, it is necessary to extend this study.

References

[1] Rijck, J.J.M., Fawaz, S.A., Schijve, J., Benedictus, R., Homan, J.J., Stress Analyses of mechanically fastened joints in aircraft fuselages, 24th ICAF Symposium, 16-18 May 2007, Naples.

[2] Skorupa, M., Korbel, A., Modeling the secondary bending in riveted joint with eccentricities. The archive of mechanical engineering 2008;55:335-52.

[3] Schijve J., Some elementary calculations on secondary bending in simple lap joints. National Aerospace Laboratory, NLR, Amsterdam, Technical Report 72036; 1972.

[4] Schijve J., Campoli, G., Monaco, A., Fatigue of structures and secondary bending in structural elements, International Journal of Fatigue 2009;31:1111-1123.

[5] Korbel, A., Skorupa, M., Skorupa, A., Machniewicz, T., Observations and analyses of secondary bending for riveted lap joints, International Journal of Fatigue 2015;72:1-10.

[6] Li, G., Johnston, A., Yanishevsky, M., Bellinger, N.C., Experimental and theoretical studies on secondary bending of bonded composite butt joint in tension, 18th AIAA/ASME/ASCE/AHS/ASC Structures, Structural Dynamics, and Materials Conference, 12-15 April 2010, Orlando, Florida.

[7] Rijck, J.J.M., Stress analysis of fatigue cracks in mechanically fastened joints, Doctor Thesis, Delft University of Technology, 2005.

[8] Niu, M.C.Y, Airframe structural design, Conmilit Press Ltd. 1988. 616 p.

Email Address

dr.willy.mendonca@gmail.com

Copyright Statement